Coordinated Beam Selection in Millimeter Wave Multi-User MIMO Using Out-of-Band Information

Flavio Maschietti, David Gesbert, Paul de Kerret
Communication Systems Department, EURECOM, Sophia-Antipolis, France
Email: {flavio.maschietti, david.gesbert, paul.dekerret}@eurecom.fr

***Abstract*—Using out-of-band (OOB) side-information has recently been shown to accelerate beam selection in single-user millimeter wave (mmWave) massive MIMO (m-MIMO) communications. In this paper, we propose a novel OOB-aided beam selection framework for a mmWave uplink multi-user system. In particular, we exploit spatial information extracted from lower (sub-6 GHz) bands in order to assist with an inter-user coordination scheme at mmWave bands. Our strategies consider the existence of a low-rate direct device-to-device (D2D) link between suitable pairs of users (UEs), enabling some information exchange. The decentralized coordination mechanism allows the suppression of the so-called co-beam interference which would otherwise lead to irreducible interference at the base station (BS) side, thereby triggering substantial spectral efficiency (SE) gains.**

I. Introduction

The large bandwidths available at mmWave carrier frequencies are expected to help meet the throughput requirements for future mobile networks [1]. In order to guarantee appropriate link margins and coverage in response to stronger path losses [2], m-MIMO antennas are expected to be used at both BS and UE sides (when the form factor allows). However, the high cost and power consumption of the radio components limits the practical implementation of a fully-digital beamforming architecture [1]. As a consequence, mixed analog-digital *(hybrid)* architectures have been proposed [3], where a low-dimensional digital processor is concatenated with an RF analog beamformer, implemented through phase shifters.

Interestingly, most works on such architectures opt to leave aside multi-user interference issues in the analog domain and cope with them in the digital part instead. For instance, in [4], the analog stage is intended to find the best beam directions at each UE regardless of the fact that resulting paths arriving at the BS from different UE might end up in the same receive BS analog beam (so-called *co-beam* interference). Yet, multiple *closely-located* UEs run the risk of sharing one or more common reflectors, causing the potential alignment of some strong paths' angles of arrival (AoA) at the BS [2]. In this case, the application of the Zero-Forcing (ZF) criterion on the resulting effective channel in the digital domain might not be effective due to the limited number of digital chains.

To solve the irreducible uplink co-beam interference problem, a possible approach consists in addressing the interference before it takes place, i.e. the UE side, as is done e.g. in [5]. Although showing significant gains over the existing solutions, such works assume perfect CSI for analog beamforming, which might not be realistic in some mmWave contexts [4].

To go around this problem, we propose a UE *coordination mechanism* exploiting statistical OOB information. Several prior works have pioneered the idea of exploiting side-information (in particular, extracted from sub-6 GHz bands) for mmWave performance optimization [6], [7], but – to our best knowledge – not in the multi-user setting. The coordination mechanism is based on the idea of each UE *autonomously* selecting an analog beam for transmission so as to strike a trade-off between (i) capturing enough channel gain and (ii) ensuring the UE signals impinge on distinct beams at the BS side. The intuition behind point (ii) is to ensure that the effective channel matrix seen by the BS preserves full rank properties, thus enabling inter-UE interference mitigation in the digital domain.

In this paper, further novelty originates from (i) the way OOB-based side-information is exploited in order to enable a coordination mechanism between the UEs, and the fact that (ii) not all UEs need to be endowed with the same amount of side-information. In particular, our scheme leverages a hierarchical information exchange which allows halving of the overall information overhead compared with a full exchange scenario.

II. System Model and Problem Formulation

We consider a multi-band scenario, where a conventional wireless network using sub-6 GHz bands coexists with a mmWave one. In the following, we introduce the mmWave model. In line with [7], the sub-6 GHz model is likewise defined, with all variables underlined to distinguish them.

A. Uplink Millimeter Wave Model

The BS is equipped with $N_{\text{BS}} \gg 1$ antennas to support K UEs with $N_{\text{UE}} \gg 1$ antennas each. The UEs are assumed to reside in a disk of radius r, which will be used to control inter-UE average distance. To ease the notation, we assume that the BS has K RF chains available (one for each UE), connected to all the N_{BS} antennas (fully-connected[1] hybrid architecture [1]).

The u-th UE precodes the data $x^u \sim \mathcal{CN}(0,1)$ with the analog unit norm vector $\mathbf{v}^u \in \mathbb{C}^{N_{\text{UE}} \times 1}$. We assume that the UEs have one RF chain each, i.e. UEs are limited to analog beamforming via phase shifters (constant-magnitude elements) [3]. In addition, $\mathbb{E}[\|\mathbf{v}^u x^u\|^2] \leq 1$, assuming normalized power constraints.

[1] Although *partially-connected* architectures are more relevant for practical implementation due to less stringent hardware requirements [8], we assume *fully-connected* architectures to keep notation light, as in most prior works focusing on mmWave SE maximization, e.g. [3]–[5]. The beam selection strategies which we will propose in Section III are in principle extendible to all mixed analog/digital beamforming architectures.

The reconstructed signal after mixed analog/digital combining at the BS is expressed as follows:

$$\hat{\mathbf{x}} = \mathbf{W}_\mathrm{D}\sum_{u=1}^{K}\mathbf{W}_\mathrm{RF}^\mathrm{H}\mathbf{H}^u\mathbf{v}^u x^u + \mathbf{W}_\mathrm{D}\mathbf{W}_\mathrm{RF}^\mathrm{H}\mathbf{n} \tag{1}$$

where $\mathbf{H}^u \in \mathbb{C}^{N_\mathrm{BS}\times N_\mathrm{UE}}$ is the channel matrix from the u-th UE to the BS, $\mathbf{n} \sim \mathcal{CN}(\mathbf{0},\sigma_\mathbf{n}^2\mathbf{I})$ is the thermal noise vector, $\mathbf{W}_\mathrm{RF} \in \mathbb{C}^{N_\mathrm{BS}\times K}$ contains the beamformers relative to each RF chain (subject to the same hardware constraints as described above), and $\mathbf{W}_\mathrm{D} \in \mathbb{C}^{K\times K}$ denotes the digital combining matrix.

Introducing the effective channel $\mathbf{h}_\mathrm{e}^u = \mathbf{W}_\mathrm{RF}^\mathrm{H}\mathbf{H}^u\mathbf{v}^u \in \mathbb{C}^{K\times 1}$ of the u-th UE, we can write (1) as follows:

$$\hat{\mathbf{x}} = \mathbf{W}_\mathrm{D}\sum_{u=1}^{K}\mathbf{h}_\mathrm{e}^u x^u + \mathbf{W}_\mathrm{D}\tilde{\mathbf{n}} = \mathbf{W}_\mathrm{D}\mathbf{H}_\mathrm{e}\mathbf{x} + \mathbf{W}_\mathrm{D}\tilde{\mathbf{n}} \tag{2}$$

where $\mathbf{H}_\mathrm{e} \in \mathbb{C}^{K\times K}$ denotes the effective channel matrix – containing all the single effective channels – and where $\tilde{\mathbf{n}} = \mathbf{W}_\mathrm{RF}^\mathrm{H}\mathbf{n}$ denotes the filtered thermal noise vector.

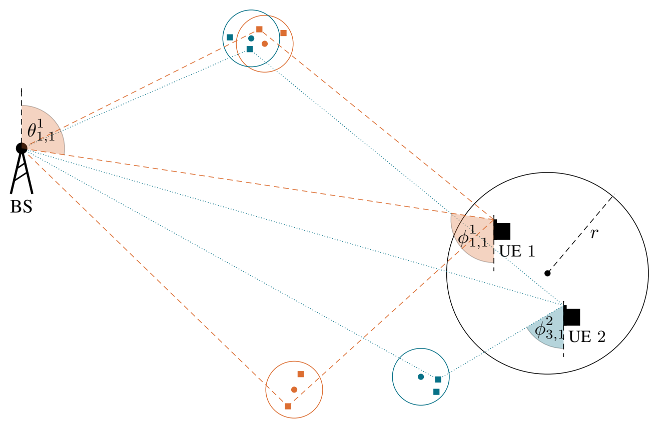

Fig. 1: Co-beam interference example with $C=3$ clusters, $L=2$ paths, and $K=2$ UEs. In this illustration, two *closely-located* UEs share some reflectors and the signal waves reflecting on the top ones arrive quasi-aligned at the BS – i.e. captured with the same BS beam – while originating from distinct UEs.

B. Channel Model

Assuming mmWave channels exhibit limited scattering [2], we adopt a geometric narrowband channel model with C clusters, each one contributing to L paths. The channel matrix $\mathbf{H}^u \in \mathbb{C}^{N_\mathrm{BS}\times N_\mathrm{UE}}$ for the u-th UE is thus expressed as follows [7]:

$$\mathbf{H}^u \triangleq \sqrt{N_\mathrm{BS}N_\mathrm{UE}}\left(\sum_{c=1}^{C}\sum_{\ell=1}^{L}\alpha_{c,\ell}^u\mathbf{a}_\mathrm{BS}(\theta_{c,\ell}^u)\mathbf{a}_\mathrm{UE}^\mathrm{H}(\phi_{c,\ell}^u)\right) \tag{3}$$

where $\alpha_{c,\ell}^u \sim \mathcal{CN}(0,\sigma_c^2)$ denotes the complex gain for the ℓ-th path of the c-th cluster of the u-th UE, including the shaping filter and the large-scale pathloss. The variables $\phi_{c,\ell}^u \in [0,2\pi)$ and $\theta_{c,\ell}^u \in [0,2\pi)$ are the AoD and AoA for the ℓ-th path of the c-th cluster connecting the u-th UE to the BS. The vectors $\mathbf{a}_\mathrm{UE}(\cdot) \in \mathbb{C}^{N_\mathrm{UE}\times 1}$ and $\mathbf{a}_\mathrm{BS}(\cdot) \in \mathbb{C}^{N_\mathrm{BS}\times 1}$ denote the antenna *unitary* steering vectors at the u-th UE and the BS, respectively. We assume *uniform linear arrays* (ULA) with $\lambda/2$ inter-element spacing.

C. Analog Codebooks

We define the codebooks used for analog beamforming as

$$\mathcal{V} \triangleq \{\mathbf{v}_1,\ldots,\mathbf{v}_{M_\mathrm{UE}}\}, \quad \mathcal{W} \triangleq \{\mathbf{w}_1,\ldots,\mathbf{w}_{M_\mathrm{BS}}\} \tag{4}$$

where $M_\mathrm{UE} = N_\mathrm{UE}$ and $M_\mathrm{BS} = N_\mathrm{BS}$ denote the number of elements (beamforming vectors) in the codebooks, and where $\mathcal{V}$ is assumed to be shared between all the UEs, to ease the notation.

For instance, with ULA, a suitable design for the fixed elements in the codebook consists in selecting steering vectors over a discrete grid of angles, as follows [4]:

$$\mathbf{v}_n = \mathbf{a}_\mathrm{UE}(\hat{\phi}_n), \quad n \in [\![1, M_\mathrm{UE}]\!] \tag{5}$$

$$\mathbf{w}_m = \mathbf{a}_\mathrm{BS}(\hat{\theta}_m), \quad m \in [\![1, M_\mathrm{BS}]\!] \tag{6}$$

where the quantized angles $\hat{\phi}_n$ and $\hat{\theta}_m$ can be chosen according to different sampling strategies of the $[0,\pi]$ range [6].

Remark 1. The notation $[\![1, M]\!]$ denotes the set $\{1,\ldots,M\}$. The same notation will be used in the remainder. □

D. Problem Formulation

The beam selection problem in mmWave communications consists in selecting the analog transmit and receive beams from $\mathcal{V}$ and $\mathcal{W}$ to maximize the sum-rate defined as follows:

$$R(\mathbf{n},\mathbf{m}) \triangleq \sum_{u=1}^{K}\log_2\big(1+\gamma^u(\mathbf{n},\mathbf{m})\big) \tag{7}$$

where $\mathbf{n} \triangleq [n_1 \quad \ldots \quad n_K]$ (resp. $\mathbf{m} \triangleq [m_1 \quad \ldots \quad m_K]$) is the vector containing the selected beams at the UE (resp. BS side), while γ^u is the received SINR for the u-th UE, defined as [4]

$$\gamma^u(\mathbf{n},\mathbf{m}) \triangleq \frac{|\mathbf{w}_\mathrm{D}^u\mathbf{h}_\mathrm{e}^u|^2}{\sum_{w\neq u}|\mathbf{w}_\mathrm{D}^u\mathbf{h}_\mathrm{e}^w|^2 + \|\mathbf{w}_\mathrm{D}^u\|^2\sigma_{\tilde{\mathbf{n}}}^2} \tag{8}$$

with $\mathbf{w}_\mathrm{D}^u \in \mathbb{C}^{1\times K}$ denoting the u-th row of $\mathbf{W}_\mathrm{D}$.

In order to maximize (7), the mutual optimization of both analog and digital components must be considered. A common viable approach consists in decoupling the design, as the analog precoder can be optimized through long-term statistical information, whereas the digital one can be made dependent on instantaneous one [4]. The same approach is followed here. In particular, we consider ZF combining, so that we have

$$\mathbf{W}_\mathrm{D} = \left(\mathbf{H}_\mathrm{e}^\mathrm{H}\mathbf{H}_\mathrm{e}\right)^{-1}\mathbf{H}_\mathrm{e}^\mathrm{H}. \tag{9}$$

The received SINR for the u-th UE is then simplified as

$$\gamma^u(\mathbf{n},\mathbf{m}) = \frac{1}{\sigma_{\tilde{\mathbf{n}}}^2\left\{\left(\mathbf{H}_\mathrm{e}^\mathrm{H}\mathbf{H}_\mathrm{e}\right)^{-1}\right\}_{u,u}}. \tag{10}$$

with the notation $\{\cdot\}_{u,u}$ denoting the u-th element on the diagonal of $\left(\mathbf{H}_\mathrm{e}^\mathrm{H}\mathbf{H}_\mathrm{e}\right)^{-1}$, associated to the u-th UE.

In general, the *perfect* knowledge of the effective channels plus a *centralized* operator to instruct the UEs are needed to maximize (7) via (10). Such information is not available without a significant resource overhead. In the next section, we propose some strategies to exploit sub-6 GHz information for a distributed and low-overhead approach to the problem.

III. Out-of-Band-Aided Beam Selection

Let us consider the existence of a sub-6 GHz channel $\utilde{\mathbf{H}}^u \in \mathbb{C}^{\utilde{N}_{\mathrm{BS}} \times \utilde{N}_{\mathrm{UE}}}$ between the u-th UE and the BS. We assume that each UE is able to compute a *spatial spectrum* $\mathbb{E}[|\utilde{\mathbf{S}}^u|^2] \in \mathbb{C}^{\utilde{M}_{\mathrm{BS}} \times \utilde{M}_{\mathrm{UE}}}$ of the sub-6 GHz channel, where [7]

$$\utilde{\mathbf{S}}^u = \utilde{\mathbf{W}}^{\mathrm{H}} \utilde{\mathbf{H}}^u \utilde{\mathbf{V}} \tag{11}$$

and where the expectation is over fast fading. The matrices $\utilde{\mathbf{W}} \in \mathbb{C}^{\utilde{N}_{\mathrm{BS}} \times \utilde{M}_{\mathrm{BS}}}$ and $\utilde{\mathbf{V}} \in \mathbb{C}^{\utilde{N}_{\mathrm{UE}} \times \utilde{M}_{\mathrm{UE}}}$ collect all the sub-6 GHz steering vectors at the BS and UE sides, sampled at the same angles as the mmWave ones. In particular, we assume $\utilde{N}_{\mathrm{BS}} \ll \utilde{M}_{\mathrm{BS}} = M_{\mathrm{BS}}$ and $\utilde{N}_{\mathrm{UE}} \ll \utilde{M}_{\mathrm{UE}} = M_{\mathrm{UE}}$. The $(\utilde{m},\utilde{n})$-th element of $\mathbb{E}[|\utilde{\mathbf{S}}^u|^2]$ contains thus the sub-6 GHz channel gain obtained with the $\utilde{n}$-th beam at the u-th UE and the $\utilde{m}$-th one at the BS.

Remark 2. The computation of $\mathbb{E}[|\utilde{\mathbf{S}}^u|^2]$ is *merely* bound to the knowledge of the average sub-6 GHz channel, as $\utilde{\mathbf{W}}$ and $\utilde{\mathbf{V}}$ are predefined fixed matrices. Note that the acquisition of the CSI matrix for conventional sub-6 GHz communications is a standard operation [9]. In this respect, sub-6 GHz channel measurements can be collected and stored *periodically* – e.g. within the channel coherence time – to be *readily* available for evaluating $\mathbb{E}[|\utilde{\mathbf{S}}^u|^2]$. In other words, obtaining the spatial spectrum $\mathbb{E}[|\utilde{\mathbf{S}}^u|^2]$ requires no additional training overhead [7]. □

A. Exploiting Sub-6 GHz Information

The available sub-6 GHz spatial information can be exploited to obtain a rough estimate of the angular characteristics of the mmWave channel. Indeed, due to the larger beamwidth of sub-6 GHz beams, one sub-6 GHz beam can be associated to a set of mmWave beams, as defined below.

Definition 1. *For a given sub-*6 *GHz beam pair* $(\utilde{n},\utilde{m})$*, we introduce the set* $\mathcal{S}(\utilde{n},\utilde{m}) \triangleq \mathcal{S}_{\mathrm{UE}}(\utilde{n}) \times \mathcal{S}_{\mathrm{BS}}(\utilde{m})$ *where* $\mathcal{S}_{\mathrm{UE}}(\utilde{n})$ *(resp.* $\mathcal{S}_{\mathrm{BS}}(\utilde{m})$*) contains all the mmWave beams belonging to the* 3*-dB beamwidth of the* $\utilde{n}$*-th (resp.* $\utilde{m}$*-th) sub-*6 *GHz beam.*

It is important to remark that we focus in this work on the selection of sub-6 GHz beams to further refine. We indeed adhere to the well-known two-stage beamforming and training operation, where *fine-grained* training (called beam refinement) follows *coarse-grained* training (called sector sweeping). In our approach, coarse-grained beam selection is achieved without *actually* training the beams with reference signals, but using instead beam information extracted from lower channels, so as to speed up the process. Once these coarse sub-6 GHz beams are chosen, the small subset of associated mmWave beams is trained. We refer to [10] for more details on this standard step. In what follows, we propose some multi-user beam selection strategies leveraging the described OOB-related side-information.

B. Uncoordinated Beam Selection

We first describe here an approach based on [4], where the authors proposed to design the analog beamformers so as to maximize the received power (SNR) for each UE, neglecting multi-user interference. When OOB information is available, the beam selection $(\utilde{n}_u^{\mathrm{un}} \in \utilde{\mathcal{V}}, \utilde{m}_u^{\mathrm{un}} \in \utilde{\mathcal{W}})$ at the u-th UE – which we will denote as *uncoordinated* (un) – can be expressed as follows:

$$(\utilde{n}_u^{\mathrm{un}}, \utilde{m}_u^{\mathrm{un}}) = \underset{\utilde{n}_u, \utilde{m}_u}{\operatorname{argmax}} \log_2\left(1 + \mathbb{E}_{n_u, m_u | \utilde{n}_u, \utilde{m}_u}\left[\gamma_{\mathrm{su}}^u(n_u, m_u)\right]\right) \tag{12}$$

where we have approximated the rate via Jensen's inequality and we have defined the single-user expected SNR, conditioned on a given sub-6 GHz beam pair $(\utilde{n}_u, \utilde{m}_u) \in \utilde{\mathcal{V}} \times \utilde{\mathcal{W}}$, as follows:

$$\mathbb{E}_{n_u, m_u | \utilde{n}_u, \utilde{m}_u}\left[\gamma_{\mathrm{su}}^u(n_u, m_u)\right] = \sum_{(n_u, m_u) \in \mathcal{S}(\utilde{n}_u, \utilde{m}_u)} \frac{g_{n_u, m_u}}{S_u \sigma_{\tilde{\mathbf{n}}}^2} \tag{13}$$

with

$$g_{n_u, m_u} \triangleq \mathbb{E}\left[\left|\mathbf{w}_{m_u}^u \mathbf{H}^u \mathbf{v}_{n_u}^u\right|^2\right] \tag{14}$$

$$= \mathbb{E}\left[\left|\mathbf{S}_{n_u, m_u}^u\right|^2\right] \tag{15}$$

being the average gain obtained at the u-th UE with the transmit-receive beam pair (n_u, m_u), and where $S_u \triangleq \mathrm{card}(\mathcal{S}(\utilde{n}_u, \utilde{m}_u))$.

In order to solve (13), the u-th UE requires an estimate of the mmWave gain g_{n_u, m_u} $\forall (n_u, m_u) \in \mathcal{S}(\utilde{n}_u, \utilde{m}_u)$. This information is not available but can be replaced for algorithm derivation purposes[2] with the gain observed in the sub-6 GHz channel over the beam pair $(\utilde{n}_u, \utilde{m}_u)$. In other words, we assume

$$g_{n_u, m_u} \approx \mathbb{E}\left[\left|\utilde{\mathbf{S}}_{\utilde{n}_u, \utilde{m}_u}^u\right|^2\right] \; \forall (n_u, m_u) \in \mathcal{S}(\utilde{n}_u, \utilde{m}_u). \tag{16}$$

Note that the average gain information derived from $\utilde{\mathbf{S}}$ will *unlikely* match with its mmWave counterpart in absolute terms practice, due to multipath, noise effects and pathloss discrepancies. Still, high correlation has been observed between the temporal and angular characteristics of the LOS path in sub-6 GHz and mmWave channels [11]. The correlation diminishes as the LOS condition is lost, as small scattering objects participating in the radio propagation emerge at higher frequencies [12]. Nevertheless, it has been shown in [13] that, in an outdoor scenario with strong reflectors (buildings), the paths with uncommon AoA at frequencies far apart[3] are less than 10% of the overall paths. In this respect, (16) allows to spot a valuable candidate set for mmWave beams in most of the situations.

Yet, an important limitation of this approach is that each UE solves its own beam selection problem *independently* of the other UEs, thus ignoring the possible impairments in terms of interference. Therefore, *as the inter-UE average distance decreases*, the performance of this procedure degrades since the UEs have much more chance to share their best propagation paths – which results in co-beam interference at the BS.

[2] The proposed algorithms are then evaluated in Section IV under realistic multi-band channel conditions as proposed in [7], where the described behavior and consequent randomness is taken into account.

[3] In [13], 5 carrier frequencies ranging between 900 MHz and 90 GHz have been compared.

C. Hierarchical Coordinated Beam Selection

In order to achieve coordination, we propose to use a hierarchical information structure requiring small overhead. In particular, an *(arbitrary)* order among the UEs is established[4], for which the u-th UE has access to the beam decisions carried out at the (lower-ranked) UEs $1,...,u-1$. This configuration is obtainable through e.g. dedicated D2D channels in the lower bands[5]. We further assume that such exchanged beam information is *perfectly* decoded at the intended UEs.

Since the UEs exchange beam indexes (in the order of few bits), the communication overhead is kept low. Moreover, the so-called *beam coherence time* – which depends on beam width and UE speed among others – has been reported to be much longer than the channel coherence time [15]. As a consequence, such overhead is only generated at long intervals.

Remark 3. Exchanging sub-6 GHz beams rather than mmWave ones introduces some *uncertainty*, but allows to save time as no UE has to wait for another one to perform beam training, i.e. the most time-consuming task in the mmWave set-up phase. □

Assuming that the sub-6 GHz beam indices $\underline{m}_{1,...,u-1}$ have been received, the *coordinated* (co) sub-6 GHz beam pair $(\underline{n}_u^{\text{co}} \in \underline{\mathcal{V}}, \underline{m}_u^{\text{co}} \in \underline{\mathcal{W}})$ at the u-th UE is obtained through solving the following optimization problem:

$$\begin{aligned}(\underline{n}_u^{\text{co}}, \underline{m}_u^{\text{co}}) &= \\ &\underset{\underline{n}_u, \underline{m}_u}{\operatorname{argmax}} \log_2\left(1 + \mathbb{E}_{\mathbf{n},\mathbf{m}|\underline{n}_u, \underline{m}_{1,...,u+1}}\left[\gamma^u(\mathbf{n},\mathbf{m})\right]\right). \end{aligned} \tag{17}$$

Solving (17) is not trivial, as it is a subset selection problem for which a Monte-Carlo approach to approximate the expectation (with a discrete summation) leads to unpractical computational time. Interestingly, for large N_{BS} and N_{UE}, we are able to derive an approximate expression for the expectation in (17). This will allow for a SINR expression similar to (13), but taking multi-user interference into account. We start with showing the following intermediate result.

Proposition 1. *In the limit of large N_{BS} and N_{UE}, the expected SINR (averaged over small-scale fading) of the u-th UE obtained after ZF combining at the BS is*

$$\mathbb{E}\left[\gamma^u(\mathbf{n},\mathbf{m})\right] = \begin{cases} \dfrac{g_{n_u,m_u}}{\sigma_{\tilde{\mathbf{n}}}^2} & \text{if } m_u \neq m_w \ \forall w \in \mathcal{K}\backslash\{u\} \\ 0 & \text{if } \exists\ w \in \mathcal{K}\backslash\{u\} : m_w = m_u \end{cases} \tag{18}$$

where we have defined $\mathcal{K} \triangleq [\![1, K]\!]$.

Proof. Based on the result in [16], we assume that the quantized angles $\hat{\phi}_n, n \in [\![1, M_{\text{UE}}]\!]$ and $\hat{\theta}_m, m \in [\![1, M_{\text{BS}}]\!]$ are spaced according to the inverse cosine function. The following lemma states an interesting consequence (constant inner product) of such a spacing which will be also useful in the remainder.

[4]The hierarchical information exchange is proposed here to facilitate the coordination mechanism at reduced overhead. In this paper, we shall leave aside further analysis on how such a *hierarchy* is defined and maintained.

[5]D2D communications allows to exchange information among *closely-located* UEs with low power and latency [14]. In particular, the power consumption for exchanging low-rate beam information over D2D could be negligible due to the small relative path loss as compared to communicating to the BS.

Lemma 1. *Let the angles $\hat{\phi}_n$ and $\hat{\theta}_m$ be spaced according to the inverse cosine function, as follows:*

$$\begin{aligned} \hat{\phi}_n &= \arccos\left(1 - \frac{2(n-1)}{M_{\text{UE}}-1}\right), \quad n \in [\![1, M_{UE}]\!] \\ \hat{\theta}_m &= \arccos\left(1 - \frac{2(m-1)}{M_{\text{BS}}-1}\right), \quad m \in [\![1, M_{BS}]\!], \end{aligned} \tag{19}$$

then

$$\begin{aligned} \mathbf{a}_{\text{UE}}^{\text{H}}(\hat{\phi}_n)\mathbf{a}_{\text{UE}}(\hat{\phi}_{\tilde{n}}) &= 1/N_{\text{UE}} \\ \mathbf{a}_{\text{BS}}^{\text{H}}(\hat{\theta}_m)\mathbf{a}_{\text{BS}}(\hat{\theta}_{\tilde{m}}) &= 1/N_{\text{BS}} \end{aligned} \tag{20}$$

for any $n \neq \tilde{n}$ and $m \neq \tilde{m}$.

According to Lemma 1, in the limit of large N_{BS} and N_{UE}, $\mathbf{a}_{\text{UE}}(\hat{\phi}_n) \perp \text{span}(\mathbf{a}_{\text{UE}}(\hat{\phi}_{\tilde{n}})\ \forall \tilde{n} \neq n)$. Likewise $\mathbf{a}_{\text{BS}}(\hat{\theta}_m) \perp \text{span}(\mathbf{a}_{\text{BS}}(\hat{\theta}_{\tilde{m}})\ \forall \tilde{m} \neq m)$. As a consequence, the matrices

$$\hat{\mathbf{A}}_{\text{BS}} = \left[\mathbf{a}_{\text{BS}}(\hat{\theta}_1) \quad \ldots \quad \mathbf{a}_{\text{BS}}(\hat{\theta}_{M_{\text{BS}}})\right], \tag{21}$$

and

$$\hat{\mathbf{A}}_{\text{UE}} = \left[\mathbf{a}_{\text{UE}}(\hat{\phi}_1) \quad \ldots \quad \mathbf{a}_{\text{UE}}(\hat{\phi}_{M_{\text{UE}}})\right] \tag{22}$$

are *asymptotically unitary*. To go further, we resort to the channel approximation in [17], which consists in approximating the channel given in (3) using the quantized angles, as follows:

$$\mathbf{H}^u \approx \sqrt{N_{\text{BS}} N_{\text{UE}}} \left(\sum_{n=1}^{M_{\text{UE}}} \sum_{m=1}^{M_{\text{BS}}} \psi_{n,m}^u \mathbf{a}_{\text{BS}}(\hat{\theta}_m) \mathbf{a}_{\text{UE}}^{\text{H}}(\hat{\phi}_n)\right) \tag{23}$$

where $\psi_{n,m}^u$ is equal to the sum of the gains of the paths whose angles lie in the *virtual spatial bin* centered on $(\hat{\phi}_n, \hat{\theta}_m)$.

We rewrite now (10) using the Schur complement as follows:

$$\gamma^u(\mathbf{n},\mathbf{m}) = \frac{1}{\sigma_{\tilde{\mathbf{n}}}^2}\left[(\mathbf{h}_{\text{e}}^u)^{\text{H}} \mathbf{h}_{\text{e}}^u - (\mathbf{h}_{\text{e}}^u)^{\text{H}} \mathbf{P}_{\text{e}/u} \mathbf{h}_{\text{e}}^u\right] \tag{24}$$

where $\mathbf{P}_{\text{e}/u} \triangleq \mathbf{H}_{\text{e}/u}(\mathbf{H}_{\text{e}/u}^{\text{H}} \mathbf{H}_{\text{e}/u})^{-1} \mathbf{H}_{\text{e}/u}^{\text{H}}$ is the orthogonal projection onto the $\text{span}(\mathbf{H}_{\text{e}/u})$, with $\mathbf{H}_{\text{e}/u}$ being the submatrix obtained via removing the u-th column from $\mathbf{H}_{\text{e}}$.

Since $\hat{\mathbf{A}}_{\text{UE}}$ and $\hat{\mathbf{A}}_{\text{BS}}$ are asymptotically unitary, it holds that

$$\mathbf{P}_{\text{e}/u} \mathbf{h}_{\text{e}}^u = \begin{cases} \mathbf{0} & \text{if } m_u \neq m_w \ \forall w \in \mathcal{K}\backslash\{u\} \\ \mathbf{h}_{\text{e}}^u & \text{if } \exists\ w \in \mathcal{K}\backslash\{u\} : m_w = m_u \end{cases} \tag{25}$$

and, as a consequence, equation (24) becomes

$$\gamma^u(\mathbf{n},\mathbf{m}) = \begin{cases} \dfrac{\|\mathbf{h}_e^u\|^2}{\sigma_{\tilde{\mathbf{n}}}^2}, & \text{if } m_u \neq m_w \ \forall w \in \mathcal{K}\backslash\{u\} \\ 0 & \text{if } \exists\ w \in \mathcal{K}\backslash\{u\} : m_w = m_u \end{cases} \tag{26}$$

whose expected value is as (18), which concludes the proof. □

Remark 4. In the large-dimensional regime, the dependence of the SINR in (8) on the transmit beams of the other UEs vanishes. In particular, catastrophic co-beam interference is experienced through intersections at the BS receive beam *only*. We kept the dependence in (18) to avoid further notation. □

Using Proposition 1, the expectation in (17) can be approximated as follows:

$$\mathbb{E}_{\mathbf{n},\mathbf{m}|\underline{n}_u,\underline{m}_{1,\dots,u}}\left[\gamma^u(\mathbf{n},\mathbf{m})\right] \approx \sum_{\substack{(n_u,m_u)\in\mathcal{S}(\underline{n}_u,\underline{m}_u) \\ m_u\notin\cup_{i=1}^{u-1}\mathcal{S}_{\mathrm{BS}}(\underline{m}_i)}} \frac{g_{n_u,m_u}}{S_u\sigma^2_{\tilde{\mathbf{n}}}}. \quad (27)$$

Using (27) in (17) to choose the sub-6 GHz beams at the u-th UE allows to take into account the *potential* co-beam interference transferred to the lower-ranked UEs with low complexity.

Remark 5. The hierarchical structure has an important role in ensuring fairness among the UEs. For example, the K-th (highest-ranked) UE has to consider via (27) the coarse-grained beam decisions of all the other (lower-ranked) UEs to avoid generating potential co-beam interference. As a consequence, such UE might be forced to exchange high communication rate for less leakage, as the best non-interfering paths might have been already taken. Therefore, it is essential to *change the hierarchy* at regular intervals to ensure an average acceptable rate per UE. This can be done e.g. through dedicated channels. □

We summarize the proposed coordinated beam selection in Algorithm 1. The algorithm is compatible with vectorization and parallelization, which minimize computational time.

Algorithm 1 OOB-Aided Hierarchical Coordinated Beam Selection at the generic u-th UE (using approximation (16))

INPUT: $\mathbb{E}\left[|\underline{\mathbf{S}}^u|^2\right]$, $\underline{m}_{1,\dots,u-1}$

Step 1: Exploiting OOB side-information

if $u=1$ **then** ▷ The u-th UE is the lowest in the *hierarchy*
  $\mathbb{E}\left[\boldsymbol{\gamma}^u\right]=\mathbb{E}\left[|\underline{\mathbf{S}}^u|^2\right]/\sigma^2_{\tilde{\mathbf{n}}}$ ▷ Solve (12) via (13)
else ▷ The u-th UE is *not* the lowest in the *hierarchy*
  for $\underline{n}=1:M_{\mathrm{UE}}$ **do**
    for $\underline{m}=1:M_{\mathrm{BS}}$ **do**
      $N=\mathrm{card}\big(\mathcal{S}(\underline{n},\underline{m}) \setminus \mathcal{S}_{\mathrm{BS}}(\underline{m}_1)\cup\cdots\cup\mathcal{S}_{\mathrm{BS}}(\underline{m}_{u-1})\big)$
      $S=\mathrm{card}\big(\mathcal{S}(\underline{n},\underline{m})\big)$
      $T=\mathbb{E}\left[|\underline{\mathbf{S}}^u_{\underline{n},\underline{m}}|^2\right]/\sigma^2_{\tilde{\mathbf{n}}}$
      $\mathbb{E}\left[\gamma^u(\underline{n},\underline{m})\right]=NT/S$ ▷ Solve (17) via (27)
    end for
  end for
end if
return $(\underline{n}^{\mathrm{co}}_u,\underline{m}^{\mathrm{co}}_u)\leftarrow\mathrm{argmax}_{\underline{n},\underline{m}}\ \mathbb{E}\left[\boldsymbol{\gamma}^u\right]$

Step 2: Pilot-training the subset of mmWave beams

$(n^{\mathrm{co}}_u,m^{\mathrm{co}}_u)\leftarrow\mathrm{argmax}_{n,m}\left|\mathbf{w}^u_m\mathbf{H}^u\mathbf{v}^u_n\right|^2\ \forall n,m\in\mathcal{S}(\underline{n}^{\mathrm{co}}_u,\underline{m}^{\mathrm{co}}_u)$

IV. Simulation Results

We evaluate here the performance of the proposed algorithm for $K=5$ *closely-located* UEs. We assume $N_{\mathrm{BS}}=64$, $N_{\mathrm{UE}}=16$ for mmWave communications, and $\underline{N}_{\mathrm{BS}}=8$ and $\underline{N}_{\mathrm{UE}}=4$ for sub-6 GHz ones. As for the carrier frequencies, we consider 28 GHz and 3 GHz for mmWave and sub-6 GHz operation, respectively. All the plotted data rates are the averaged – over 10000 Monte-Carlo iterations – instantaneous sum-rates, obtained after ZF combining at the digital stage (BS side).

A. Multi-Band Channels

The performance of the proposed OOB-aided algorithms depends on the *spatial congruence* between sub-6 GHz and mmWave channels. The authors in [7] proposed a simulation environment for generating sub-6 GHz and mmWave channels based on the model in (3). The MATLAB®code used to simulate those channels is open-source and available on IEEEXplore [7]. We use the same model except that we consider a narrowband channel model, for which path time spread and beam squint effect can be neglected [2]. Note that frequency-selective filters at the BS side helps discriminating (in time) among UEs which generate co-beam interference, and thus might results in giving an extra performance in average wideband channels. In this paper, we consider a worst case scenario to present the substance of our idea. In principle, models and algorithms could be extended to a wideband setting.

B. Results and Discussion

We consider a stronger (on average) LOS cluster with respect to the reflected ones, as the LOS is indeed the prominent propagation driver in mmWave bands [2]. In particular, we adopt the following large-scale pathloss model:

$$\mathrm{PL}(\delta)=\alpha+\beta\log_{10}(\delta)+\xi \qquad [\mathrm{dB}] \qquad (28)$$

where δ is the path length and where the pathloss parameters α, β and ξ are taken from Table 1 in [2] for both LOS and NLOS contributions. The large-scale pathloss is then reflected in the cluster power $\sigma^2_c\ \forall c$. The average power of all the paths in a given cluster is assumed to be equal. Since the model in [7] is for a single-user scenario, we consider the model in [18] to extend it so as to generate correlated channel clusters for all the neighboring UEs in the disk. In [18], the position of the clusters is made also dependent on the position of the UEs, and as a result, the possible sharing of reflectors and scatterers for neighboring UEs is taken into account. An example of the available sub-6 GHz spatial spectrum at two UEs is shown in Fig. 2.

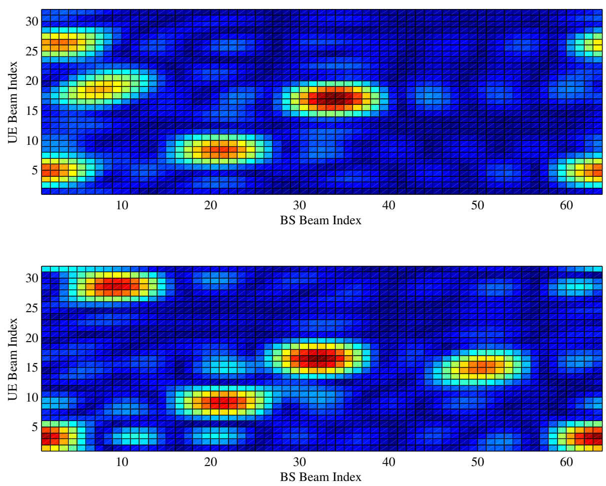

Fig. 2: Example of available $\mathbb{E}[|\underline{\mathbf{S}}^u|^2]$ at two neighboring UEs, with $r=11$ m. Some reflectors are being shared, while others are uncommon. The average path gains can be different.

In Fig. 3, we show the sum-rate of the proposed algorithms as a function of the SNR, where the average distance between the UEs is 13 meters. For reference, we also plot the curve related to the upper bound achieved with no multi-user interference. The proposed OOB-aided coordinated algorithm outperforms the uncoordinated one, which neglects co-beam interference.

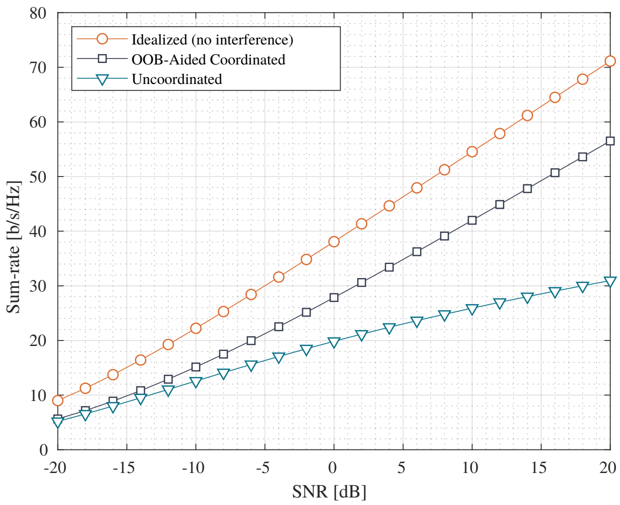

Fig. 3: Sum-rate vs SNR. The average inter-UE distance is 13 m. The OOB-aided coordinated algorithm outperforms the uncoordinated one. The coordination gain increases with the SNR.

In Fig. 4, we show the sum-rate of the proposed algorithms as a function of the average inter-UE distance, for a mmWave SNR of 1 dB. The coordination among the UEs allows for huge SE gains for inter-UE distances below 15 meters. As the average inter-UE distance increases – and so, there is less chance for the co-beam interference to occur – the performance gap between the two algorithms narrows.

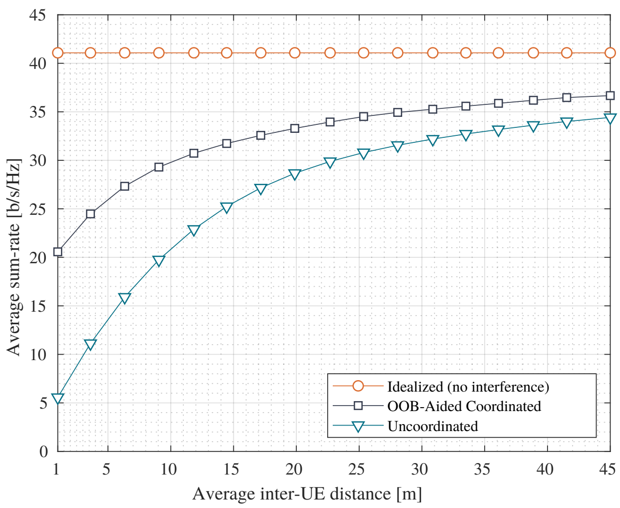

Fig. 4: Sum-rate vs average inter-UE distance. The SNR is fixed to 1 dB. The performance gain achieved through coordination decreases with the inter-UE distance.

V. Conclusions

In mmWave communications, suitable strategies for interference minimization can be applied in the beam domain through e.g. exploiting spatial side-information. In this work, we introduced a low-overhead OOB-aided decentralized beam selection algorithm for a mmWave uplink multi-user scenario, leading to improved interference management. Finding clear relationships between mmWave and lower bands radio environments is essential for OOB-aided approaches – in particular, towards robust algorithms taking channels discrepancies into account – and it is an interesting research problem which is still open as well.

VI. Acknowledgment

The authors are supported by the ERC under the EU's H2020 research program (Agreement no. 670896 PERFUME).

References

[1] R. W. Heath, N. González-Prelcic, S. Rangan, W. Roh, and A. M. Sayeed, "An overview of signal processing techniques for mmwave MIMO systems," *IEEE J. Sel. Top. Signal Process.*, Apr. 2016.

[2] M. R. Akdeniz, Y. Liu, M. K. Samimi, S. Sun, S. Rangan, T. S. Rappaport, and E. Erkip, "Millimeter wave channel modeling and cellular capacity evaluation," *IEEE J. Sel. Areas Commun.*, June 2014.

[3] A. Alkhateeb, O. E. Ayach, G. Leus, and R. W. Heath, "Channel estimation and hybrid precoding for mmwave cellular systems," *IEEE J. Sel. Top. Signal Process.*, Oct. 2014.

[4] A. Alkhateeb, G. Leus, and R. W. Heath, "Limited feedback hybrid precoding for multi-user millimeter wave systems," *IEEE Trans. Wireless Commun.*, Nov. 2015.

[5] Y. Zhu and T. Yang, "Low complexity hybrid beamforming for uplink multiuser mmwave MIMO systems," in *Proc. IEEE WCNC*, Mar. 2017.

[6] F. Maschietti, D. Gesbert, P. de Kerret, and H. Wymeersch, "Robust location-aided beam alignment in millimeter wave massive MIMO," *Proc. IEEE GLOBECOM*, Dec. 2017.

[7] A. Ali, N. González-Prelcic, and R. W. Heath, "Millimeter wave beam-selection using out-of-band spatial information," *IEEE Trans. Wireless Commun.*, Feb. 2018.

[8] S. Park, A. Alkhateeb, and R. W. Heath, "Dynamic subarrays for hybrid precoding in wideband mmwave MIMO systems," *IEEE Trans. Wireless Commun.*, May 2017.

[9] 3GPP, "NR; physical layer procedures for data - Rel. 15," TS 38.214. Dec. 2018.

[10] J. Kim and A. F. Molisch, "Fast millimeter-wave beam training with receive beamforming," *IEEE J. Commun. Netw.*, Oct. 2014.

[11] C. K. Anjinappa and I. Guvenc, "Angular and temporal correlation of v2x channels across sub-6 ghz and mmwave bands," in *Proc. IEEE ICC Workshops*, May 2018.

[12] V. Raghavan, A. Partyka, A. Sampath, S. Subramanian, O. H. Koymen, K. Ravid, J. Cezanne, K. Mukkavilli, and J. Li, "Millimeter-wave MIMO prototype: measurements and experimental results," *IEEE Commun. Mag.*, Jan. 2018.

[13] A. Ali, N. González-Prelcic, and R. W. Heath, "Estimating millimeter wave channels using out-of-band measurements," in *Proc. IEEE ITA*, Jan. 2016.

[14] J. Chen, H. Yin, L. Cottatellucci, and D. Gesbert, "Feedback mechanisms for FDD massive MIMO with D2D-based limited CSI sharing," *IEEE Trans. Wireless Commun.*, Aug. 2017.

[15] V. Va, J. Choi, and R. W. Heath, "The impact of beamwidth on temporal channel variation in vehicular channels and its implications," *IEEE Trans. Veh. Technol.*, Jun. 2017.

[16] H. Q. Ngo, E. G. Larsson, and T. L. Marzetta, "Aspects of favorable propagation in massive MIMO," in *Proc. IEEE EUSIPCO*, Sept. 2014.

[17] A. M. Sayeed, "Deconstructing multiantenna fading channels," *IEEE Trans. Signal Process.*, Oct. 2002.

[18] S. S. Mahmoud, Z. M. Hussain, and P. O'Shea, "A space-time model for mobile radio channel with hyperbolically distributed scatterers," *IEEE Antennas and Wireless Propagation Letters*, Dec. 2002.